

correlation for the channel with square ribs (case B), is given by

$$R(e^+) = 3.23, \quad 2541 \geq e^+ \geq 415 \quad (5)$$

The channel with full circular ribs (case C) yields the highest  $R$  value of 3.9. It is evident that the friction roughness function is independent of the roughness Reynolds number for all of the cases studied. From the experimental values of  $R(e^+)$ ,  $f$  can be predicted using Eqs. (1), (2), and (4). The correlated value of the function  $R(e^+)$ , of the present study, is less than 1% higher than the correlated value of Han<sup>2</sup> for the channel with two square ribbed walls and  $P/e = 10$ .

The heat transfer roughness function increases with increasing roughness Reynolds number for the rib profiles. The correlation of  $G(e^+)$  for the case with square ribs of the present investigation with a deviation of  $\pm 2\%$  is given by Eq. (6):

$$G(e^+) = 1.891(e^+)^{0.381}, \quad 2541 \geq e^+ \geq 415 \quad (6)$$

These results compare well with Han<sup>2</sup> for a channel with square ribs on two ribbed walls, and with Chandra and Cook<sup>3</sup> for a similar channel, but  $P/e = 8$ . For a given rib configuration and flow Reynolds number, the heat transfer coefficient can be predicted from the experimental values of  $G(e^+)$  and Eqs. (1), (3), and (4).

### Conclusions

1) The regionally averaged Nusselt number ratio decreases with increasing Reynolds number and is almost a constant value in the fully developed region of the channel.

2) The heat transfer enhancement increases with surface roughness, 2.53 with square ribs to 2.01 (a 26% decrease) with semicircular ribs, for  $Re = 3.6 \times 10^4$ .

3) The friction factor ratio increases with increasing Reynolds number. The minimum friction occurs with full circular ribs, and the maximum with square ribs. The heat transfer performance decreases with increasing Reynolds number.

4)  $R(e^+)$  is independent of  $e^+$ , and the value with square ribs compares well with Han.<sup>2</sup>

5)  $G(e^+)$  increases with increasing  $e^+$ , and decreases for turbulators with sharp corners. The channel with slant-edged ribs has the lowest heat transfer roughness function. The correlation of the function compares well with Han<sup>2</sup> and Chandra and Cook.<sup>5</sup>

6) The experimental data may be applied to the design of equipment that require internal cooling channels with two ribbed walls with nonrectangular rib profiles.

### References

- <sup>1</sup>Han, J. C., "Heat Transfer and Friction in Channels with Two Opposite Rib-Roughened Walls," *Journal of Heat Transfer*, Vol. 106, No. 4, 1984, pp. 774–781.
- <sup>2</sup>Han, J. C., "Heat Transfer and Friction Characteristics in Rectangular Channels with Rib Turbulators," *Journal of Heat Transfer*, Vol. 110, No. 2, 1988, pp. 321–328.
- <sup>3</sup>Han, J. C., Zhang, Y. M., and Lee, C. P., "Augmented Heat Transfer in Square Channels with Parallel, Crossed, and V-Shaped Angled Ribs," *Journal of Heat Transfer*, Vol. 113, No. 3, 1991, pp. 590–596.
- <sup>4</sup>Metzger, D. E., and Vedula, R. P., "Heat Transfer in Triangular Channels with Angled Roughness Ribs on Two Walls," *Experimental Heat Transfer*, Vol. 1, No. 1, 1987, pp. 31–44.
- <sup>5</sup>Chandra, P. R., and Cook, M. M., "Effect of the Number of Channel Ribbed Walls on Heat Transfer and Friction Characteristics of Turbulent Flows," *Proceedings of the AIAA/ASME 6th Thermophysics and Heat Transfer Conference*, HTD-Vol. 271, AIAA, Washington, DC, 1994, pp. 201–209.
- <sup>6</sup>Chandra, P. R., Niland, M. E., and Han, J. C., "Turbulent Flow Heat Transfer in a Rectangular Channel with Varying Number of Ribbed Walls," *Journal of Turbomachinery*, Vol. 119, No. 2, 1997, pp. 374–380.

<sup>7</sup>Liou, T. M., and Hwang, J. J., "Effect of Ridge Shapes on Turbulent Heat Transfer and Friction in a Rectangular Channel," *International Journal of Heat and Mass Transfer*, Vol. 36, No. 4, 1993, pp. 931–940.

<sup>8</sup>Taslim, M. E., and Spring, S. D., "Effect of Turbulator Profile and Spacing on Heat Transfer and Friction in a Channel," *Journal of Thermophysics and Heat Transfer*, Vol. 8, No. 3, 1994, pp. 555–562.

<sup>9</sup>Kline, S. J., and McClintock, F. A., "Describing Uncertainties in Single Sample Experiments," *Mechanical Engineering*, Vol. 75, Jan. 1953, pp. 3–8.

## View-Factor Evaluation by Quadrature over Triangles

C. K. Krishnaprakas\*

ISRO Satellite Centre, Bangalore 560 017, India

### Introduction

THE need to evaluate radiation view factors often arises in thermal, illumination, and optical engineering practices. View factor between two finite surfaces is obtained as the solution of a double area integral. In the case of simple geometries, the solution can be obtained through analytical integration, and formulas are presented in Refs. 1–4. Howell<sup>5</sup> presented a catalog that contains view factors in terms of closed-form expressions for many geometries. However, complex geometries do not permit an analytical solution and, hence, the view-factor integral or its contour-integral representation should be evaluated by numerical means or statistical sampling techniques.<sup>1–4</sup> Chung and Kim<sup>6</sup> demonstrated the application of the finite element method (FEM) in the numerical estimation of view factors. Ambirajan and Venkateshan<sup>7</sup> presented a general method based on a contour-integral representation using the trapezoidal rule of numerical integration in conjunction with the Romberg extrapolation technique to get an accurate result. Ambirajan and Venkateshan<sup>7</sup> also resolved the problem of logarithmic singularity encountered along the common edge of two surfaces by analytically evaluating the integral. In a more recent paper, Rao and Sastri<sup>8</sup> extended the contour-integral technique to treat curved surfaces with the aid of a nonlinear transformation to map the boundaries and used the Gaussian quadrature for an accurate evaluation of the integral. This Note describes a method of numerical evaluation of view factors using the Gaussian quadrature over triangles. The advantage is that surfaces of more general shape can be better approximated by a set of triangles rather than by any other shaped area elements. Moreover, quadrature over triangles is also easier to use.

### Radiation View Factor

The radiation view factor between two finite surfaces  $i$  and  $j$  is defined as the fraction of diffusely radiated energy leaving surface  $i$  that is directly incident on surface  $j$ , and is mathematically expressed as

$$F_{ij} = \frac{1}{A_i} \int_{A_i} \int_{A_j} \frac{\cos \theta_i \cos \theta_j dA_i dA_j}{\pi r^2} \quad (1)$$

Where  $\theta_i$  and  $\theta_j$  are the angles between the surface normals and the line connecting two points, respectively, on the two

Received March 5, 1997; revision received June 9, 1997; accepted for publication Sept. 18, 1997. Copyright © 1997 by the American Institute of Aeronautics and Astronautics, Inc. All rights reserved.

\*Engineer, Thermal Systems Group.

surfaces.  $A_i$  and  $A_j$  are the surface areas in question, and  $r$  is the length of the connecting line. If numerical integration is used for Eq. (1), the surfaces may be subdivided into a number of elements, and view-factor algebra can be used to arrive at the final view factor from the elemental view factors.

### Numerical Scheme

Geometrical ideas from the theory of FEM may now be applied to evaluate Eq. (1) numerically. Chung and Kim<sup>6</sup> demonstrated the application of FEM by dividing the surfaces into quadrilateral elements. The relationship between the local and global coordinate systems is established through the direction cosines of the local axes with respect to the global axes. The variation of the global coordinates is related to the nodal values through the use of isoparametric shape functions. This mapping enables the integration over the quadrilateral to be converted to the integration over a square in isoparametric coordinates, and the one-dimensional Gaussian quadrature rule in product form is applied. However, this method of Chung and Kim<sup>6</sup> leads to the formation of four nested loops of summation in the process of integration and, hence, needs more evaluations of the integrand.

Surfaces of general shape can be better approximated by the assembly of a number of triangles rather than quadrilaterals. Moreover, integration rules over triangles are convenient to use and require fewer sampling points. Sufficiently higher-order integration rules over triangles are available in literature.<sup>9,10</sup> The use of area coordinates for quadrature over triangles reduces the number of summation loops from four to two.

Let us consider the view factor between two triangles arbitrarily placed in the three-dimensional space (Fig. 1). The global coordinate of a point on a triangle can be related to the nodal values at the three vertices through the area coordinates as  $x(\mathbf{L}) = \mathbf{L}^T \mathbf{x}$ ,  $y(\mathbf{L}) = \mathbf{L}^T \mathbf{y}$ , and  $z(\mathbf{L}) = \mathbf{L}^T \mathbf{z}$ , where  $\mathbf{L}$  = area coordinate vector =  $(L_1, L_2, L_3)^T$ ,  $\mathbf{x}$  =  $x$  coordinate vector =  $(x_1, x_2, x_3)^T$ ,  $\mathbf{y}$  =  $y$  coordinate vector =  $(y_1, y_2, y_3)^T$ , and  $\mathbf{z}$  =  $z$  coordinate vector =  $(z_1, z_2, z_3)^T$ . Subscripts to the area coordinates refer to the components, and global coordinates refer to the vertices of the triangle. Superscript  $t$  refers to transpose of the vector.  $L_i$  is the ratio of the area of the triangle formed by the point of interest, and the other two vertices ( $j$  and  $k$ ) of the triangle, i.e.,  $L_1$  = area of triangle P23/area of triangle 123,  $L_2$  = area of triangle P13/area of triangle 123, etc. (Fig. 1). The components of  $\mathbf{L}$  follow the identity  $L_1 + L_2 + L_3 = 1$ . The elemental area  $dA$  is mapped into area coordinates as  $dA = |J| dL_1 dL_2$ , where  $J$  is the Jacobian matrix of the coordinate transformation.<sup>11</sup>

With the preceding coordinate mapping and using Eq. (1), the view factor between triangles 1 and 2 is written as

$$F_{12} = \frac{1}{\pi A_1} \int_{A_1} \int_{A_2} f(\mathbf{L}^1, \mathbf{L}^2) dL_1^1 dL_2^1 dL_1^2 dL_2^2 \quad (2)$$

where

$$f(\mathbf{L}^1, \mathbf{L}^2) = \frac{|J^1||J^2| \cos \theta_1 \cos \theta_2}{r^2} \quad (3)$$

Superscripts to  $\mathbf{L}$  and  $J$  refer to the elements in question. For the evaluation of a two-dimensional integral over the triangle, the following Gaussian quadrature rule is used:

$$I = \int_{\Delta} \int_{\Delta} f(\mathbf{L}) dL_1 dL_2 = \frac{1}{2} \sum_{i=1}^n w_i f(\mathbf{L}_i) \quad (4)$$

where  $w_i$  and  $\mathbf{L}_i$  are, respectively, the weights and sampling points of the  $n$ -point quadrature rule.<sup>9,10</sup>

Employing Eq. (4) in Eq. (2) results in

$$F_{12} = \frac{1}{4\pi A_1} \sum_{i=1}^n \sum_{j=1}^n w_i w_j f(\mathbf{L}^{1i}, \mathbf{L}^{2j}) \quad (5)$$

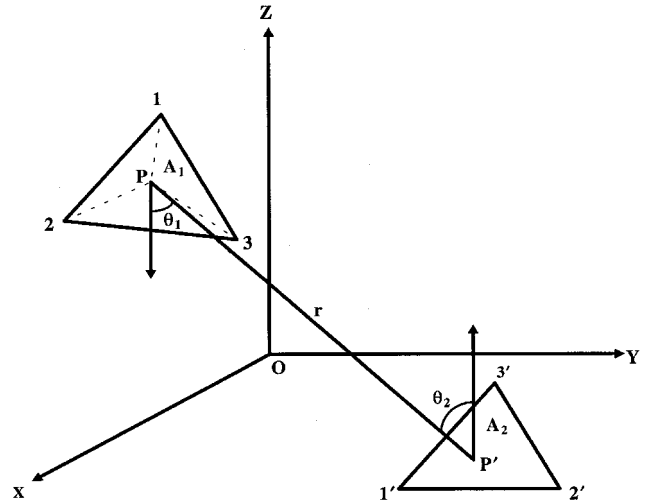


Fig. 1 Orientation of two triangles in three-dimensional space.

Note that Eq. (5) involves only two nested loops of summation as compared to four for the method described by Chung and Kim.<sup>6</sup> Now, when evaluating the view factor between two general surfaces,  $i$  and  $j$ , the surfaces may be divided into a number of triangular elements, and the elemental view factors are assembled to arrive at  $F_{ij}$  as

$$F_{ij} = \frac{1}{A_i} \sum_{k=1}^M \sum_{l=1}^N A_{ik} F_{ikjl} \quad (6)$$

where  $F_{ikjl}$  is the elemental view factor between the triangle  $ik$  on surface  $i$  and  $jl$  on surface  $j$ , obtained using Eq. (5);  $A_{ik}$  is the area of  $ik$ ; and  $M$  and  $N$  are, respectively, the number of triangular divisions on  $i$  and  $j$ .

### Results and Discussion

Equation (6) is applied to the configurations of directly opposing parallel regular polygons of unit side length kept apart at a unit distance; the solutions have been presented by Howell.<sup>5</sup> Five quadrature schemes, employing 1, 3, 4, 7, and 13 sampling points were tried. All of the computations were performed on an IBM PC-AT/386 in single-precision arithmetic. The results are shown in Table 1. The mesh size number characterizing the number of triangles of equal area to which each surface was subdivided is shown in column 1. For the problem of directly opposing unit squares kept a unit distance apart, using a three-point quadrature scheme and 54 triangular divisions takes 5.1 s of CPU time, but the result is not accurate. For the same problem, accurate results are obtained by employing the 13-point scheme without any discretization in 0.83 s of CPU time. Therefore, more accurate results are obtained by a higher-order quadrature scheme than by finer discretization.

Table 2 shows the results of the configuration of two perpendicular squares having a common edge. Column 1 shows the number of triangular divisions of equal area made on each square. The method converges slowly in this case. To obtain more accurate results or quick convergence in this problem, finer discretization and more integration points are required. This is because of the  $1/r^2$  singularity of the integrand along the common edge. A quadrature scheme capable of handling singularity is called for in such situations. Alternatively, contour integral representation of the view-factor integral, Eq. (1), overcomes the numerical difficulty associated with the singularity because analytical expressions are available for the line integral along the common edge.<sup>7</sup> However, incorporating the effects of intervening surfaces blocking the view between two surfaces in question is quite cumbersome to deal with using the contour integral method. In the present method, this is easily accomplished.

**Table 1 View factor between two directly opposing parallel regular polygons of unit side length kept a unit distance apart**

Number of Gaussian points on each triangle	$F_{1-2}$					
	Mesh size number, <sup>a</sup> $L$	Triangle	Square	Pentagon	Hexagon	Octagon
1	0	0.137832	0.257831	0.368130	0.464989	0.643672
	1	0.120373	0.229424	0.324090	0.405530	0.537930
	3	0.109101	0.207098	0.291471	0.363160	0.475964
3	0	0.104752	0.197475	0.277149	0.345880	0.461233
	1	0.105346	0.199069	0.279319	0.347319	0.455020
	3	0.105581	0.199746	0.280328	0.348383	0.454768
4	0	0.104128	0.196185	0.276504	0.347001	0.476499
	1	0.105026	0.198469	0.278528	0.346927	0.457669
	3	0.105527	0.199622	0.280151	0.348185	0.454665
7	0	0.105657	0.199926	0.280526	0.348552	0.454960
	1	0.105625	0.199868	0.280492	0.348552	0.454842
	3	0.105614	0.199841	0.280483	0.348595	0.455009
13	0	0.105605	0.199824	0.280474	0.348615	0.455173
	1	0.105606	0.199825	0.280466	0.348587	0.455040
	3	0.105606	0.199825	0.280463	0.348579	0.455016
	Howell <sup>5</sup>	0.105604	0.199825	0.280465	0.346849 <sup>b</sup>	0.455024

<sup>a</sup>The number of triangles to which each polygon is discretized equals  $M = N = (m - 2)3^L$ , where  $m$  is the number of sides of the polygon.

<sup>b</sup>An evaluation by the contour-integral method yielded the value as 0.348576; in close agreement with the value obtained by the present method.

**Table 2 View factor between perpendicular squares having a common edge**

Number of triangular divisions	$F_{12}$ <sup>a</sup> number of Gaussian points		
	4	7	13
2	0.321624	0.309306	0.288867
6	0.333847	0.324938	0.322096
18	0.255293	0.244418	0.242321
54	0.252433	0.221894	0.218808
162	0.235106	0.216049	0.213402
486	0.227757	0.210508	0.208769
1458	0.218589	0.207387	0.206187

<sup>a</sup>Exact value = 0.200044.

The usefulness of the method basically lies in handling irregular geometries rather than computational speed. The speed of the method may be enhanced by employing an adaptive quadrature scheme such that finer mesh is used only at difficult regions, otherwise a coarser mesh may be attempted.<sup>12-14</sup> The method is useful for radiation heat transfer analysis based on the finite element method.

### Acknowledgments

The author is grateful to D. R. Bhandari, Head, Thermal Design and Analysis Division; V. K. Kaila, Group Head; H. Narayanamurthy, Group Director, Thermal Systems Group; and A. V. Patki, Deputy Director, of the ISRO Satellite Centre for their support and encouragement during the course of this work.

### References

- <sup>1</sup>Sparrow, E. M., and Cess, R. D., *Radiation Heat Transfer*, Augmented Edition, Hemisphere, Washington, DC, 1978.
- <sup>2</sup>Siegel, R., and Howell, J. R., *Thermal Radiation Heat Transfer*, Hemisphere, Washington, 1992.
- <sup>3</sup>Brewster, M. Q., *Thermal Radiative Transfer and Properties*, Wiley, New York, 1992.
- <sup>4</sup>Modest, M. F., *Radiative Heat Transfer*, McGraw-Hill, New York, 1993.
- <sup>5</sup>Howell, J. R., *A Catalog of Radiation Configuration Factors*, McGraw-Hill, New York, 1982, p. 119.
- <sup>6</sup>Chung, T. J., and Kim, J. Y., "Radiation View Factors by Finite Elements," *Journal of Heat Transfer*, Vol. 104, Nov. 1982, pp. 792-795.
- <sup>7</sup>Ambirajan, A., and Venkateshan, S. P., "Accurate Determination of Diffuse View Factors Between Planar Surfaces," *International Journal of Heat and Mass Transfer*, Vol. 36, No. 8, 1993, pp. 2203-2208.
- <sup>8</sup>Rao, V. R., and Sastri, V. M. K., "Efficient Evaluation of Diffuse View Factors for Radiation," *International Journal of Heat and Mass Transfer*, Vol. 39, No. 6, 1996, pp. 1281-1286.
- <sup>9</sup>Hughes, T. J. R., *The Finite Element Method*, Prentice-Hall, Englewood Cliffs, NJ, 1987.
- <sup>10</sup>Strang, G., and Fix, G. J., *An Analysis of the Finite Element Method*, Prentice-Hall, Englewood Cliffs, NJ, 1973.
- <sup>11</sup>Mohr, G. A., *Finite Elements for Solids, Fluids and Optimization*, Oxford Univ. Press, Oxford, England, UK, 1992.
- <sup>12</sup>Laurie, D., "Automatic Numerical Integration over a Triangle," National Research Center for Mathematical Sciences of the CSIR, Tech. Rept., Pretoria, South Africa, 1978.
- <sup>13</sup>Lyness, J. N., "AUG2-Integration Over a Triangle," Argonne National Lab. Rept., ANL/MCS-TM-13, 1983.
- <sup>14</sup>Doncker E. de, and Robinson, I., "An Algorithm for Automatic Integration over a Triangle Using Nonlinear Extrapolation," *ACM Transactions on Mathematical Software*, Vol. 10, 1984, pp. 1-16.